Biochimica et Biophysica Acta 1837 (2014) 773–781

Contents lists available at ScienceDirect

Biochimica et Biophysica Acta

journal homepage: www.elsevier.com/locate/bbabio

Spectroscopic properties of photosystem II core complexes from *Thermosynechococcus elongatus* revealed by single-molecule experiments

Marc Brecht [a,b,*], Sepideh Skandary [a], Julia Hellmich [c], Carina Glöckner [c], Alexander Konrad [a], Martin Hussels [a], Alfred J. Meixner [a], Athina Zouni [c,d], Eberhard Schlodder [c]

[a] Universität Tübingen, IPTC and Lisa + Center, Auf der Morgenstelle 18, Tübingen, Germany
[b] Zurich University of Applied Sciences, Technikumstrasse 13, 8401 Winterthur, Switzerland
[c] Technische Universität Berlin, Max-Volmer-Institut, Straße des 17. Juni 135, Berlin, Germany
[d] Humboldt Universität zu Berlin, Institut für Biologie, Philippstr. 13, 10099 Berlin, Germany

ARTICLE INFO

Article history:
Received 30 October 2013
Received in revised form 28 January 2014
Accepted 31 January 2014
Available online 6 February 2014

Keywords:
Photosystem II core complex
CP43
CP47
Single-molecule spectroscopy
Low temperature spectroscopy
Fluorescence quenching

ABSTRACT

In this study we use a combination of absorption, fluorescence and low temperature single-molecule spectroscopy to elucidate the spectral properties, heterogeneities and dynamics of the chlorophyll *a* (Chl*a*) molecules responsible for the fluorescence emission of photosystem II core complexes (PS II cc) from the cyanobacterium *Thermosynechococcus elongatus*. At the ensemble level, the absorption and fluorescence spectra show a temperature dependence similar to plant PS II. We report emission spectra of single PS II cc for the first time; the spectra are dominated by zero-phonon lines (ZPLs) in the range between 680 and 705 nm. The single-molecule experiments show unambiguously that different emitters and not only the lowest energy trap contribute to the low temperature emission spectrum. The average emission spectrum obtained from more than hundred single complexes shows three main contributions that are in good agreement with the reported bands F685, F689 and F695. The intensity of F695 is found to be lower than in conventional ensemble spectroscopy. The reason for the deviation might be due to the accumulation of triplet states on the red-most chlorophylls (e.g. Chl29 in CP47) or on carotenoids close to these long-wavelength traps by the high excitation power used in the single-molecule experiments. The red-most emitter will not contribute to the fluorescence spectrum as long as it is in the triplet state. In addition, quenching of fluorescence by the triplet state may lead to a decrease of long-wavelength emission.

© 2014 Elsevier B.V. All rights reserved.

1. Introduction

Photosystem II (PS II) is the membrane protein complex of higher plants, green algae and cyanobacteria that uses solar energy to catalyze the electron transfer from water to plastoquinone [1,2]. The photo-oxidized electron donor of PS II ($P680^+$) is one of the most powerful oxidizing species capable of driving the oxidation of water to oxygen. The structure of dimeric PS II core complexes (PS II cc) from cyanobacteria has been determined by X-ray crystallography to a resolution of up to 1.9 Å [3,4]. Fig. 1 shows the chlorophyll containing subunits of PS II cc according to the structural model at 2.9 Å resolution [4]. Subunits CP43 and CP47 contain 13 and 16 chlorophyll *a* (Chl*a*) molecules, respectively. The PS II reaction center (RC), which is formed by the subunits D1, D2 and Cyt *b559*, binds six Chl*a* and two pheophytin *a* molecules. The RC is surrounded by the subunits CP47 and CP43. The primary function of CP47 and CP43 is to harvest light and transfer the absorbed energy to the RC, where the photochemical charge separation takes place.

The optical properties of PS II cc, its individual subunits (CP43, CP47) and the RC have been studied in detail [5–15]. The shape of the fluorescence emission spectrum depends remarkably on temperature [6,7,10–13]. Two spectral components at 685 nm and 695 nm, called F685 and F695, were used to explain the temperature dependence. Andrizhiyevskaya et al. [11] concluded that F695 originates from excitations that are irreversibly transferred to the red-absorbing 690 nm chlorophylls of CP47 and that F685 originates from excitations that are slowly transferred to the RC, where they are irreversibly trapped by charge separation. At 4 K almost all excitations that reach the 690 nm chlorophylls of CP47 will remain on this chlorophyll, whereas some excitations will become trapped on the red-most chlorophylls of CP43. Information about the optical properties of CP43 and CP47 core antennae was obtained from high-resolution spectroscopy in the frequency domain [6,16]. Excitation dependent fluorescence line narrowing spectra of PS II from spinach gave first evidence that CP43 holds two emitting states with different inhomogeneous distributions at low temperatures

Abbreviations: PS I, photosystem I; PS II, photosystem II; PS II cc, photosystem II core complex; CP43 CP47, chlorophyll binding subunits of PS II; ZPL, zero-phonon line; RC, reaction center; Chl*a*, chlorophyll *a*; Car, carotenoid

* Corresponding author.
E-mail address: marc.brecht@uni-tuebingen.de (M. Brecht).

0005-2728/$ – see front matter © 2014 Elsevier B.V. All rights reserved.
http://dx.doi.org/10.1016/j.bbabio.2014.01.025

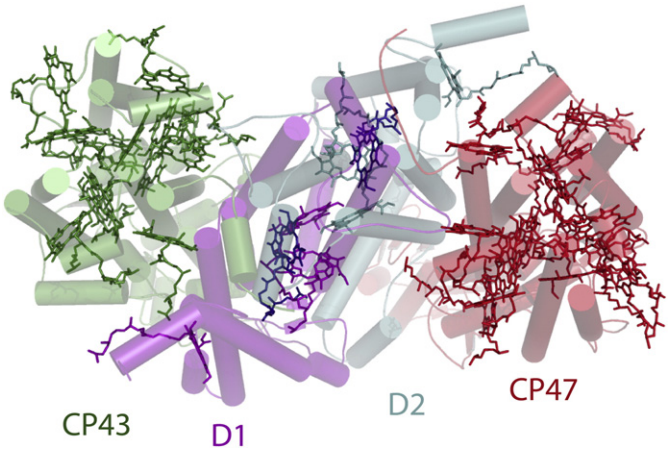

Fig. 1. Chlorophyll containing subunits of PS II cc. The Chl*a* molecules coordinated by the subunits CP43, D1, D2 and CP47 (cartoon mode) are shown in green, purple, cyan and red, respectively. The two Pheophytin (Pheo) a molecules are colored in dark blue. The figure was made with PyMol using the coordinates of the structural model of PS II cc from *Thermosynechococcus elongatus* at 2.9 Å resolution (Ref. [4], (PDB code 3BZ1)).

[6]. Komura et al. [12] performed picosecond time-resolved fluorescence spectroscopy on spinach PS II at 4, 40, and 77 K and identified an additional fluorescence band at 689 nm (F689). The fast decay of F689 suggests an energy transfer directly from F689 to P680 [12]. The complex interrelation between the different subunits and the strong influence of the inhomogeneous widths of the different red-states makes a set of optical techniques necessary to solve their function in the excitation energy transfer.

In this study we investigate the optical properties of intact, oxygen-evolving PS II cc dimers of *Thermosynechococcus elongatus* at the single-molecule level. Single-molecule techniques overcome the inhomogeneous broadening. This is especially useful if the influence of inhomogeneity is covered by ensemble averaging [17]. At ambient temperatures, the susceptibility of the chromophores to fluctuations of the protein moiety and its surrounding media leads to line broadening (spectral diffusion) [18–20]. Lowering the temperature is one possibility to reduce the impact of fluctuations on the chromophores' site energies. Low temperature experiments have the additional advantage to minimize photobleaching and limitations in the observation time [21]. Assuming that all fluctuations are suppressed, the emission profile of a single emitter composed out of a sharp zero-phonon-line (ZPL) and a phonon-wing becomes observable. The ZPL belongs to an electronic transition between the vibronic ground state of the first electronic excited state and the vibronic ground state of the electronic ground state. This kind of emission is not accompanied by the creation or annihilation of phonons. The phonon wing on the low-energy side of the ZPL is due to the reorganization of the surrounding induced by the excitation of the chromophores from the ground to the excited state. The reorganization leads to the excitation of phonons (lattice vibrational modes). Due to the small line width of the ZPLs, it is possible to observe the process of spectral diffusion in slow-motion as nicely shown by experiments on LH2 and PS I at 1.4 K [22,23]. The widths of those spectral jumps reach into the range of several nanometers indicating remarkable changes in the site energy of the emitting chlorophyll molecules. In a recent study on PS I, we were able to show that a large portion of the spectral dynamics in the lower hierarchical levels is connected to fluctuations of protons located close to the chromophores [24]. Such protons can be found e.g. in hydrogen bonds between the chromophore and nearby amino acid residues, or structural water molecules [24,25]. The consideration of site-energy changes induced by all of these fluctuations is necessary to understand the optical properties of these proteins, especially if the chromophores take part in energy transfer. Coupled chromophores are found in almost all pigment proteins that are involved in light harvesting. Then, spectral jumps of only one chromophore are able to redirect the actual pathways of a traveling exciton and as a consequence it takes influence on the function of the whole protein complex [26,27].

2. Material and methods

2.1. Single-molecule fluorescence spectroscopy

Dimeric PS II cc from *T. elongatus* have been isolated and purified as described in Ref. [28]. The purified PS II cc dimers were diluted in buffer solution containing 100 mM PIPES (pH7.0), 5 mM $CaCl_2$, 0.5 M betaine, and 0.03% β-DM. For single molecule experiments, PS II complexes were diluted in buffer to a final PS II concentration of about 3 pM. About 1 μl of this suspension was placed between cover slips made of glass. Finally the sample was transferred directly into the cryostat and rapidly plunged into liquid helium. Experiments were carried out using a home-built confocal microscope operating at 1.6 K as described recently in Ref. [29].

The excitation intensity of the laser, measured before entering the cryostat, was 100 μW resulting in a flux of approximately $6.6 \cdot 10^{20}$ photons/(cm^2 s). The excitation wavelength was 665 nm for all experiments. The highest resolution of the spectrometer (Shamrock 500 spectrograph with 200 lines/mm and 400 lines/mm gratings in combination with Andor Newton back illuminated deep depleted CCD) is ~0.05 nm. In a sequence of spectra, the usual exposure time for each spectrum is 2 s resulting in a typical S/N ratio of >6 for single PS II cc dimers at the given excitation power referred to as time resolution in the following context.

2.2. Measurement of steady state absorption and fluorescence spectra

Absorption spectra were recorded with a spectral resolution of 1 nm on a Cary-1E-UV/VIS spectrophotometer (Varian, Inc.). Fluorescence spectra were recorded in a FluorMax 2 (Jobin Yvon) photon counting spectrofluorometer. The spectra were corrected for the spectral sensitivity based on the measurement of a calibrated light source. For the measurements, PS II complexes were diluted to a final Chl concentration of about 5 μM with buffer containing 20 mM MES-NaOH (pH 6.5), 10 mM $MgCl_2$, 10 mM $CaCl_2$, 0.02% (w/w) β-DM and glycerol (final concentration about 65% (v/v)), to obtain a transparent glass at low temperatures. For experiments at cryogenic temperatures, the cuvette was placed in a variable temperature liquid nitrogen bath cryostat (Oxford DN1704) or an Oxford liquid helium flow cryostat (Oxford CF1204). A home-built cryostat holder was used in the spectrophotometer and spectrofluorometer.

3. Results and discussion

3.1. Ensemble absorption and emission spectra of PS II cc

Fig. 2 presents temperature-dependent absorption and fluorescence emission spectra of PS II cc dimers from *T. elongatus*. At 5 K the Q_Y absorption exhibits peaks at 674 nm and 684 nm and shoulders near 669 nm, 677 nm, 680 nm and 694 nm. The second derivative of the 5 K spectrum shows minima at the specified wavelengths indicating various pigment pools (not shown).

The emission band at 290 K is centered at around 683 nm. At 50 K, two bands located at 685 nm and 694 nm are resolved. These bands are generally named F685 and F695. The 20 K fluorescence spectrum exhibits the maximum at 691 nm. The overall behavior is in good agreement with measurements on PS II samples from spinach [5,11]. The band at 695 nm (F695) has been assigned to the lowest lying energy state of the chlorophylls in CP47 [5,11] that is associated with Chl29 by several groups (using the nomenclature used in Loll et al. [30]) [2,7,31,32]. Low energy chlorophylls become traps for the excitation energy, if the thermal

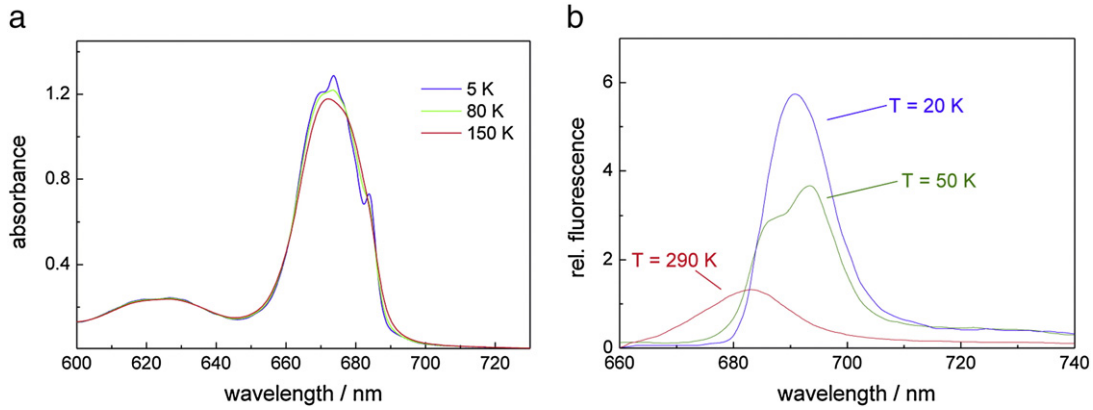

Fig. 2. (a) The panel on the left shows absorption spectra of dimeric PS II cc from *T. elongatus* at 5 K, 80 K and 150 K. The Q_y absorption band is centered at about 673 nm. (b) The panel on the right shows fluorescence spectra of dimeric PS II cc from *T. elongatus* at 20 K, 50 K and 290 K.

energy (kT) is not sufficient to enable uphill energy transfer to the RC. Lowering the temperature from 50 K to 5 K causes the fluorescence to increase and its maximum to shift to the blue to 691 nm at 20 K and 687 nm at 5 K (see Fig. 2b and Refs. [5,10–12]). This blue shift and fluorescence increase may be interpreted by the assumption that chlorophylls, absorbing at slightly shorter wavelengths than the lowest energy chlorophyll start to successively trap the excitation energy if the temperature is lowered. There are two possibilities for this case: (a) These chlorophylls are all part of the inhomogeneous distribution of transition energies of the lowest lying energy state of the chlorophylls in CP47 or (b) structurally different chlorophylls in the PS II antenna become a trap, which are not connected by fast energy transfer with the lowest state in CP47.

3.2. Emission spectra of individual PS II cc dimers

Fig. 3 shows a selection of six fluorescence emission spectra (denoted I–VI) of different single PS II cc dimers. The acquisition time for the spectra was 40 s. Single PS II cc dimers can be detected at low temperature using the fluorescence emission of several Chl*a* molecules acting as traps for the excitation energy at cryogenic temperatures with a significant fluorescence quantum yield.

The emission spectra of single PS II cc are characterized by ZPLs covering the whole range of fluorescence from 680 to 750 nm. Each spectrum exhibits unique features. In the wavelength range 680 to 690 nm all spectra show several ZPLs. Their number varies between two (spectrum VI) and six to seven (spectrum I). At wavelengths larger than 690 nm clearly visible lines are only observed in spectra I–III. Their intensities are reduced compared to the lines in the range 680–690 nm.

Fig. 4 shows a series of fluorescence emission spectra recorded on one single PS II cc within 2, 10, 50, 100 and, 200 s. The spectra show one pronounced line at ~684 nm and a line with smaller intensity at ~682 nm. The line width (fitted by a Gaussian) increases in the spectra taken at 2 and 200 s from ~0.35 nm (for both lines) to 1.15 nm (line at 682 nm) and 1.20 nm (line at 684 nm). The time dependent broadening of the lines indicates that spectral diffusion is the main underlying broadening process. Further details about the number and spectral positions of emitters responsible for the fluorescence emission of single PS II cc dimers are obtained from the analysis of their polarization. Fig. 5 shows the fluorescence emission of a single PS II cc dimer in dependence of the polarizer angle in front of the spectrograph. This angle is defined with respect to an arbitrary laboratory axis and is uncorrelated to the polarization of the excitation light [33]. In Fig. 5, the dependence of the whole emission spectra as a function of the polarizer orientation is shown. Three pronounced contributions at 684.7 nm, 686.2 nm and, 689.7 nm can be distinguished. The intensity of these contributions vanishes at specific angles almost completely; therefore a strong linear polarization can be assumed. Similar intensity variations were observed for all PS II cc investigated in this way. A strong polarization of the fluorescence emission from the different Chls requires either a single emitter as the origin of the emission or a number of emitters with parallel transition dipole moments. Since the PS II cc are randomly oriented in our samples, it is unlikely that the transition moments of several emitters would appear parallel in all cases. Therefore, the number of emitters responsible for the fluorescence emission of a single PS II cc can be determined by this method. A detailed study on this topic is in preparation.

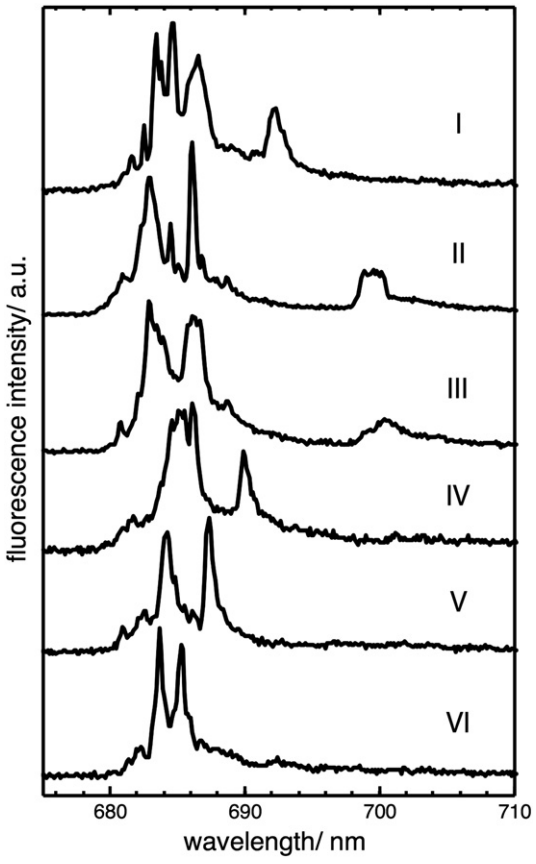

Fig. 3. Single-molecule fluorescence emission spectra from PS II cc dimers of *Thermosynechococcus elongatus*. Spectra were recorded on different individual complexes. The accumulation time was 40 s for each complex. For better comparability, the spectra that exhibited intensity differences were scaled to a similar magnitude. Excitation wavelength 665 nm; temperature 1.6 K.

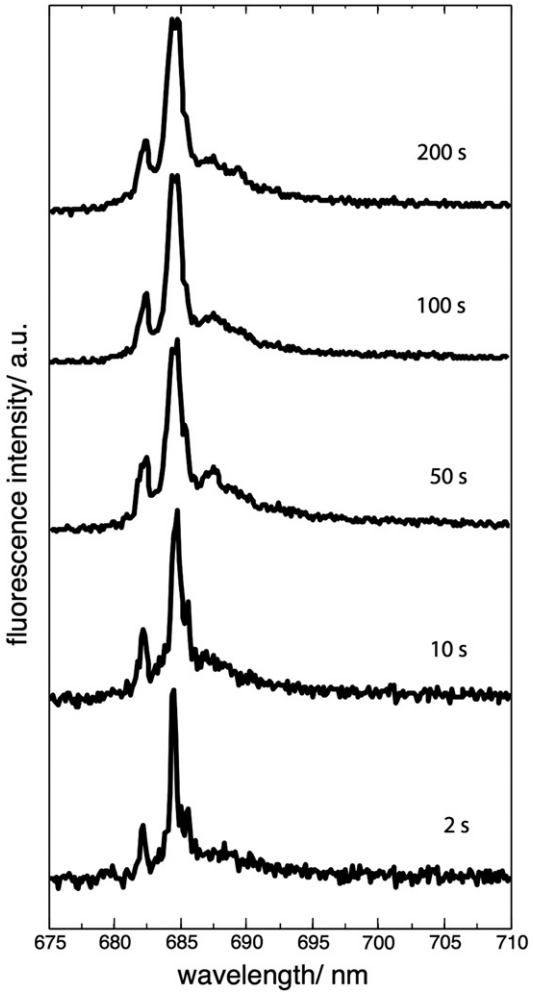

Fig. 4. Dependence of fluorescence emission spectra of one single PS II cc dimer on acquisition time. Excitation wavelength 665 nm; temperature 1.6 K.

3.3. Spectral dynamics and intensity variations of ZPLs

The basis of the dynamical process leading to the spectral broadening can be analyzed in our setup with sufficient S/N ratio using an acquisition time of 2 s. In order to analyze the spectral dynamics in the emission of PS II cc sequences of fluorescence spectra of 140 complexes were recorded. In Fig. 6 two representative examples of the time-dependent behavior of ZPLs are shown. The sequences consist of 100 spectra consecutively recorded with 2 s acquisition time. The average spectra are shown on top. The average spectrum (Fig. 6a) is dominated by two intense emitters at 682.9 nm (fwhm = 1.34 nm) and 686.2 nm (fwhm = 0.35 nm) and one broad line at 699.8 nm (fwhm = 1.66 nm). In the sequence it becomes obvious that these emitters show quite different spectral diffusion behavior. The intense line around 682.9 nm remains in the first 80 s within a limited spectral range. In the interval 100–160 s, its spectral width is expanded. Starting at 160 s up to the end of the sequence, the bandwidth is reduced again. The line around 686.2 nm remains for the most of the time at one spectral position. Only in time intervals e.g. 60–65 s, 140–148 s the line undergoes discrete jumps in frequency. In all cases the jump width is ~0.8 nm. The third line at 699.8 nm shows also pronounced spectral diffusion, but even more striking are the intensity variations of this line. In the first 80 s, the line has a low intensity. During the interval 80–150 s, the intensity is increased and the line shows several jumps in frequency until the intensity drops down completely. The sequence (Fig. 6b) shows an example for ZPLs without changes in the wavelength position during time. The average spectrum shows two intense ZPLs at 682.6 nm (fwhm = 1.0) and 684.4 nm (fwhm = 0.6) as well as a ZPL with lower intensity at 690.1 nm (fwhm = 0.6). All three lines are visible during the whole time of data acquisition. The lines at 682.6 nm and at 690.1 nm show almost no change in wavelength during time, whereas for the line at 684.4 nm slight changes are observed. Both lines show intensity variations of almost 100%, whereas the line at 690.1 nm emits with almost constant intensity.

Different lines in single-molecule spectra (e.g. see Fig. 3) may be the result of spectral diffusion (i), static disorder (ii), or different emitters (iii): (i) As can be seen in Fig. 6 spectral jumps are typically less than 1.5 nm. Lines, which are close together, may be assigned to a single emitter whose site-energy changes due to protein dynamics during the accumulation period. In general, spectral diffusion leads to a time dependent broadening of the lines (see Fig. 4) and not to separated lines. (ii) Chlorophylls bound at the same site in both monomers of the PS II dimer might have different transition energies. A Gaussian distribution is often used to describe the extent of static disorder within an ensemble with a full width at half maximum of about 200 cm^{-1} corresponding to about 10 nm [13]. (iii) Different low energy traps bound at CP43 and CP47 give rise to separated lines if the low energy states are not connected to each other by efficient energy transfer leading rapidly to thermal equilibrium. Taking the above-mentioned processes together it is reasonable that at least 2–3 emitters contribute to the emission spectra shown in Fig. 3; nevertheless an uncertainty in the determination of their correct number remains. To remove this remaining uncertainty, polarization dependent measurements (shown above) are a perfect tool to unravel overlapping signals and to account for the correct number of emitters.

The movement of the ZPLs is characterized by discrete spectral jumps with different widths and not by continuous changes in their positions (Fig. 6). A plausible explanation of the spectral dynamics observed in LH2 based on the hierarchy of tiers in the energy landscape of a protein is given in Ref. [22]. We adopt this explanation for the observed spectral dynamics in PS II. High energetic barriers between the different conformational substates characterize the highest tier in the energy landscape. Under the given low-temperature conditions, the barriers cannot be crossed and the system rests in one given conformational substate in the first tier. Two different situations are illustrated

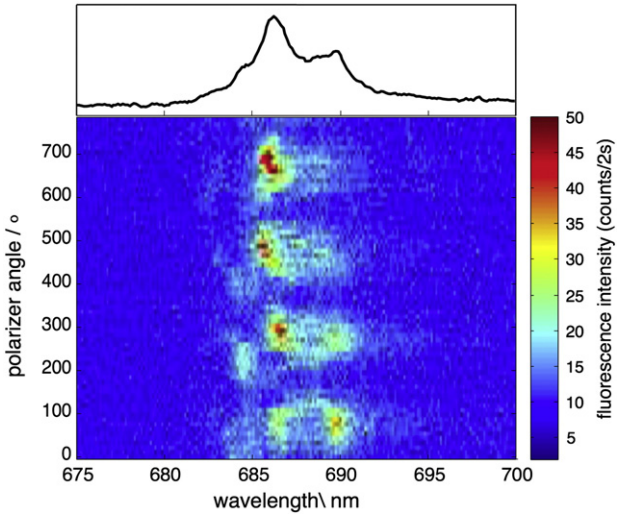

Fig. 5. Sequence of fluorescence emission spectra of a single PS II cc dimer as a function of the orientation of the polarizer in front of the spectrograph. The acquisition time was 2 s for each spectrum. Excitation wavelength 665 nm; temperature 1.6 K. The individual spectra were recorded in steps of 10°. The angle of the polarizer is shown on the left side.

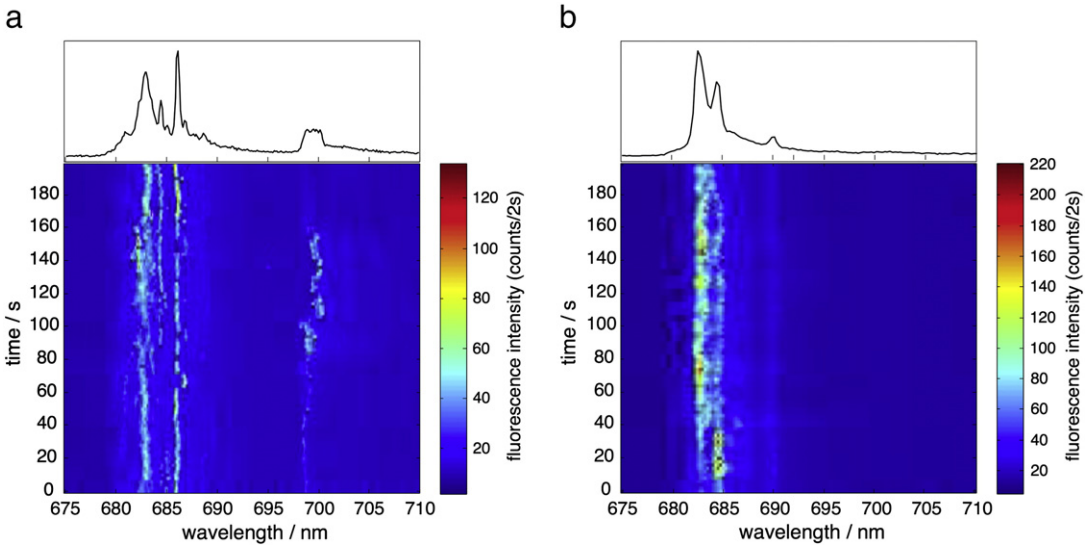

Fig. 6. Plots of time-dependent fluorescence emission spectra of single PS II cc dimers. The time sequences of 100 spectra with an accumulation time of 2 s for each spectrum are displayed for both complexes. Excitation wavelength 665 nm; temperature 1.6 K.

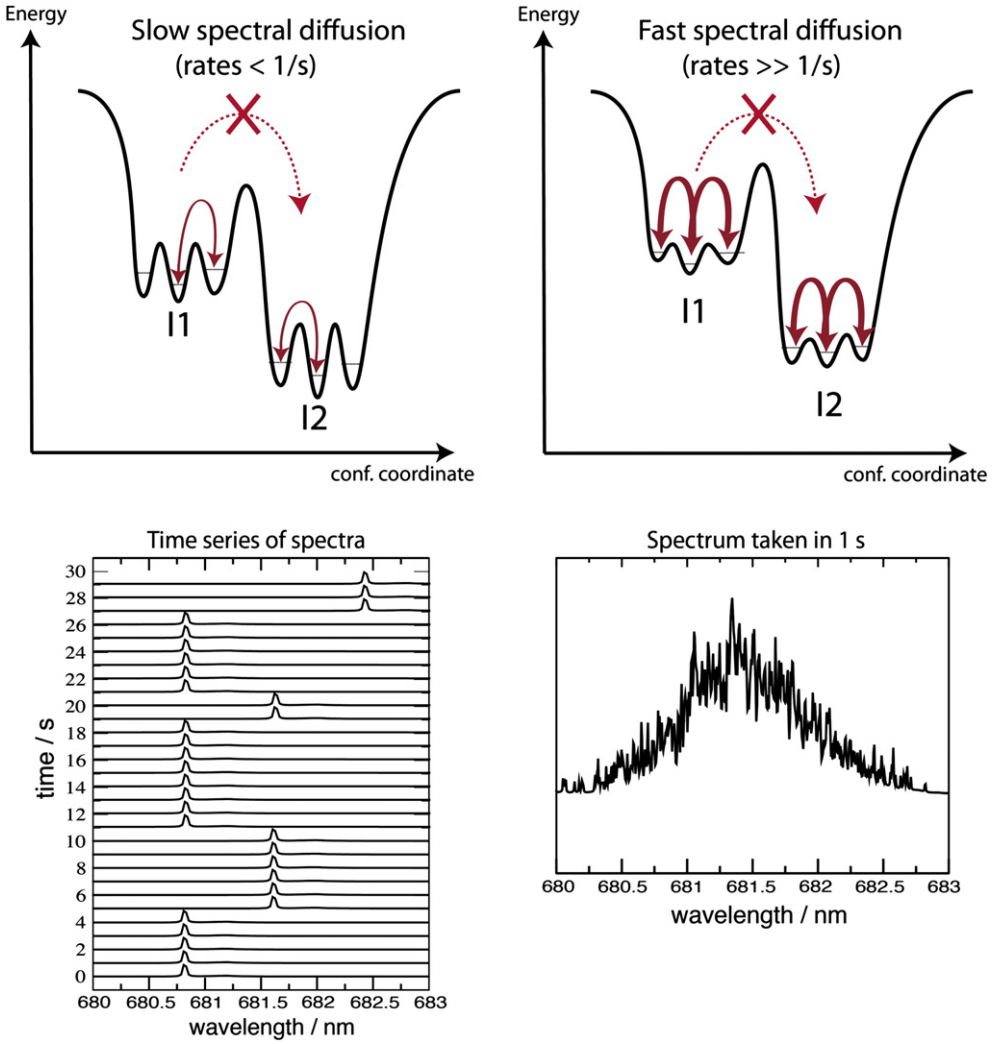

Fig. 7. Schematic illustration of the protein energy landscape. I1, I2 represent different intermediate states in the first tier. The energetic barrier between I1 and I2 cannot be crossed at low temperatures, but the barriers within I1 and I2 can be crossed (red arrows), yielding the observed jumps of the ZPLs in the emission spectra (see also Fig. 6). The barrier heights within I1 and I2 determine the rates of the conformational changes. (Left) The barriers within I1/I2 are high. Jumps occur with low rates. If the rates are in the range of the acquisition time (here ~2 s) stable ZPLs and discrete jumps can be observed in the resulting emission spectra (slow spectral diffusion). (Right) Reduced barrier heights yields increased rates, if the barriers are crossed with rates much higher than the acquisition time only broadened lines can be observed (fast spectral diffusion).

in Fig. 7. The energetic barriers between the different substates within the second tier are lower. As a consequence, these barriers can be crossed under the experimental conditions. The crossing of these barriers induces the observed line broadenings (Fig. 4) and spectral jumps (Fig. 6). The jumps are induced by small conformational changes that are possible in the second tier. Nevertheless, these changes are able to induce jumps covering a major fraction of the whole inhomogeneous line width [24]. The observation of stable ZPLs or broadened lines depends on the rates of these jumps [34].

The contributions of CP43 and CP47 are both inhomogenously broadened and their emission bands show certain overlap. The complex temperature dependence of PS II fluorescence is interpretable by noting that excitation transfer from CP43 and CP47 to the RC is slow, and strongly dependent on the precise energy at which a slow-transfer pigment in CP43 or CP47 is located within its inhomogeneous distribution [2,11,32,35]. The observed intensity variations of the emitters in Fig. 6 are most probably induced by slight changes in the site energies of the Chl*a* involved in the excitation energy transfer [26]. Especially, site-energy fluctuations of the low energy states of CP43 and CP47 will have a remarkable effect on the excitation energy transfer between the subunits and the RC.

3.4. Single-molecule average emission spectrum

As shown e.g. for PSI, the average spectrum can be reconstructed by the summation of ≥100 spectra of individual pigment protein complexes [36]. Fig. 8 shows the average emission spectrum obtained by summation of all spectra of single PS II cc dimer. The maximum fluorescence intensity is located around 685 nm. A pronounced shoulder is observed on the long-wavelength side between 690 and 695 nm. The fwhm of the peak is about 8 nm.

A satisfactory Gaussian decomposition of the average emission spectrum can be achieved by using at least three contributions (see Fig. 8). The maxima of the Gaussian bands are around 684.7, 689.3, and 691.4 nm. Vibrational contributions are taken into account by the fourth component at 701.8 nm. The overall agreement between the spectrum and the fitting function is quite good; a minor deviation is visible only at around 691 nm. The three Gaussian bands cover the wavelength regions, in which ZPLs are predominantly observed in the emission spectra of single PS II cc dimer (see Figs. 3, 5 and 6).

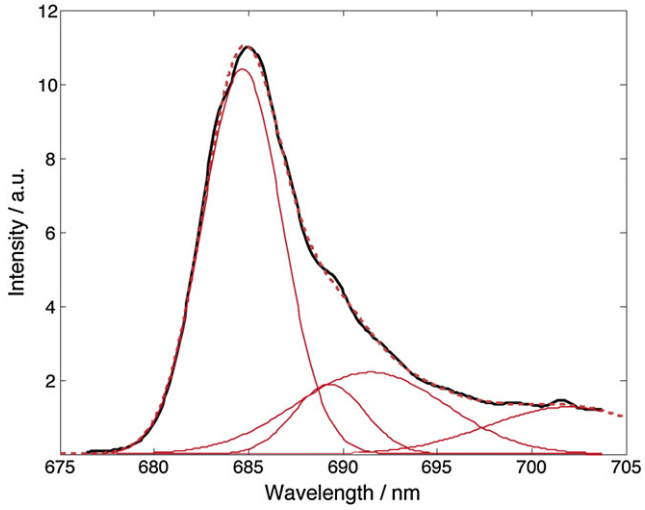

Fig. 8. The summation (average) of all fluorescence spectra taken on individual single PS II cc dimers (black) fitted by four Gaussian functions. The individual Gaussians are given in red, the summation of all Gaussians is given by the red-dotted curve. The wavelength positions and the widths of the Gaussians are: 684.7 nm/6.0 nm, 689.3 nm/5.3 nm, 691.4 nm/11.2 nm, and 701.9 nm/12.0 nm.

The contribution around 684.7 nm is in good agreement with the position of F685 assigned to a contribution from CP43 [2,11,32]. The shape of the emission spectrum shows a certain dependence on the wavelength of the excitation light. The highest intensity of the CP43 contribution was reported for excitation in the wavelength range between 665 and 673 nm [11]. In our experiment, we used 665 nm for excitation; therefore, the contributions of CP43 should also be enhanced. The second contribution is found at around 689.3 nm. The wavelength position and the width of this contribution are in good agreement with the F689 contribution reported by Komura et al. [12]. The third band is centered at around 691.4 nm. It has been proposed that the band F695 shifts from ~695 nm at 70 K to ~692 nm at 5 K [10]. This assignment can be used for the interpretation of the contributions in the single-molecule spectra e.g. Fig. 5. The weak contribution at 684.7 nm and the intense line at 686.2 nm fall into the wavelength range assigned to CP43, whereas the component with the lowest energy belongs most likely to CP47. Therefore, it can be concluded that the fluorescence of PS II results from different sites between which the energy transfer is frozen out (see Introduction section).

The complex temperature dependence of PS II fluorescence can be interpreted by noting that excitation transfer from CP43 and CP47 to the RC is slow, and strongly dependent on the precise energy at which a low-energy pigment in CP43 or CP47 is located within its inhomogeneous distribution [2]. Therefore, future single-molecule experiments will be helpful to get further insights into the influence of the inhomogeneity of the different spectral bands on the energy transfer in PS II.

The single-molecule average emission spectrum shown in Fig. 8 is significantly different from ensemble emission spectra measured by conventional fluorescence spectrometer. In ensemble experiments, the maximum emission for PS II cc was found between 687.5 nm and 690 nm below 20 K (see Fig. 2 and Refs. [10–12,37]); i.e. a few nm shifted to the red. The fwhm of the ensemble spectra is about 14 nm, i.e. nearly a factor two larger than that of the single-molecule average emission spectrum shown in Fig. 8. A notable exception is the recently reported fluorescence spectrum of PS II cc from *T. vulcanus* that was obtained by time integrals of time-wavelength 2-D images obtained with a Streak camera set-up [32]. This spectrum is virtually identical to our single-molecule average emission spectrum shown in Fig. 8. It should also be noted that emission spectra reported for the RC and CP43 from spinach PS II exhibit the maxima at 683.7 nm and 682.8 nm [6,11]. The line width of the RC is larger, whereas the line width of CP43 is close to the low value found by the single-molecule experiments.

The emission spectra of single PS II cc dimers (see Fig. 3) and the single-molecule average emission spectrum (see Fig. 8) clearly demonstrate that three or more emitters contribute to the fluorescence spectrum of PS II core complexes at low temperature. This indicates that the excitation energy is trapped at different low energy states in the PS II core antenna. Due to their low Q_Y transition energy, uphill excitation energy transfer to the RC becomes impossible at cryogenic temperatures. These states are not connected to each other by efficient energy transfer leading to thermal equilibration, because otherwise the excitation energy would be localized at 5 K on the lowest energy state being the only emitting state.

The sum of all contributions determines the shape of the fluorescence spectrum. The reason for the observed difference between the single-molecule average spectrum and the ensemble spectrum is most likely that the intensities of the contributions are different, as different quenching mechanisms might be effective under the respective conditions of the experiments.

Upon illumination at cryogenic temperatures, the light-induced formation of $P680^+Q_A^-$ in PS II is followed by charge recombination, as the electron transfer from Q_A^- to Q_B and from Y_Z to $P680^+$ is inhibited. The extent of $P680^+Q_A^-$ formation decreases progressively with

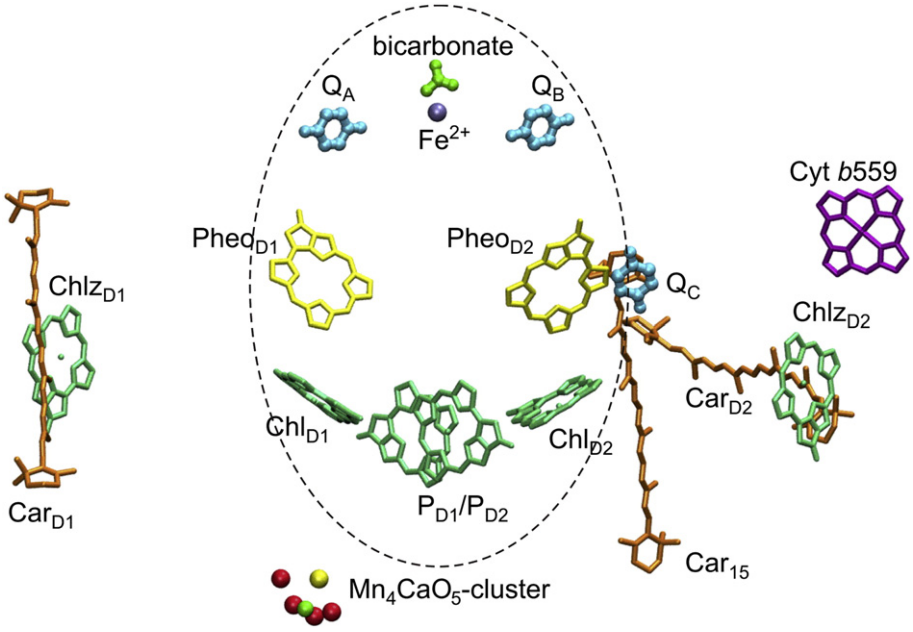

Fig. 9. Arrangement of the cofactors of the RC of PS II cc including the presumably involved co-factors of the secondary electron transfer (view perpendicular to the pseudo-C2 axis) based on the structural model of PS II cc from *T. elongatus* at 2.9 Å resolution (Ref. [4], (PDB code 3BZ1)). Shown are the two Chl*a*s constituting P680, P_{D1}/P_{D2} (green), the two peripheral Chls, Chl_{ZD1} and Chl_{ZD2} (green), the β-carotene (Car) molecules identified so far in the RC, Car (orange), and cytochrome (Cyt) b559 (violet).

successive turnovers. The reason is the oxidation of secondary electron donors (Car, Chl_Z, Cyt *b*559, Y_Z) by $P680^+$, which occurs with low quantum yield in competition to the charge recombination of $P680^+Q_A^-$. Thereby, long-living states as e.g. $Q_A^-P680Car^+$, $Q_A^-P680Cyt\ b559^+$, or $Q_A^-P680Chl_Z^+$ are accumulated after several turnovers [38]. Fig. 9 shows the arrangement of the mentioned cofactors in the X-ray structure. In the presence of Q_A^- (closed PS II), the primary radical pair $P680^+Pheo^-$ can still be formed, but stabilization of the charge separation is not possible. Fluorescence induction experiments have shown that the fluorescence yield increases upon reduction of Q_A [39,40]. The increase is stronger for PS II frozen with Cyt *b*559 in the reduced state than for PS II frozen with Cyt *b*559 oxidized. In the first case, it is $Q_A^-P680Cyt\ b559^+$, whereas in the second case, it is $Q_A^-P680Car^+$ and $Q_A^-P680Chl_Z^+$, that is predominantly accumulated upon illumination at low temperature. This difference might be due to trapped Chl^+ and Car^+, which are known to be efficient quencher of the excitation energy [41,42].

There is no need for high excitation intensities, to accumulate the discussed long-living states. Therefore, reduced Q_A and oxidized secondary donors are most likely present while measuring fluorescence spectra by conventional ensemble spectroscopy as well as single-molecule spectroscopy. Thus, the described light-induced reactions in the RC cannot explain the differences in the shape of the emission spectra (single-molecule vs. ensemble).

However, in single-molecule experiments the photon flux has to be much higher than in conventional fluorescence spectroscopy in order to achieve a satisfactory signal-to-noise ratio. In our experiments, the flux was approximately $6.6 \cdot 10^{20}$ photons/(cm^2 s). With an absorption cross section σ for PS II of about $7 \cdot 10^{-15}$ cm^2 at 665 nm, the excitation rate $\sigma \cdot I$ is of the order of 10^6 s^{-1}. A relatively high excitation power was also used for the time-resolved fluorescence measurements with the streak camera set-up by Shibata et al. [32]. With an excitation power of 0.5 W/cm^2 at 430 nm, the excitation rate is about $1.4 \cdot 10^4$ s^{-1}.

Under such conditions, the accumulation of triplet states, ^{3}Chl and ^{3}Car, in CP47 and CP43 can be expected. The structural data of PS II show that about one third of the chlorophylls in CP47 (Chl17, Chl22, Chl26, Chl27 and Chl29) as well as in CP43 (Ch33, Chl43, Chl47, and Chl49) are in close contact ($\leq$5 Å) to a β-carotene [43]. This structural information is in line with triplet-minus-singlet absorbance difference spectra of isolated CP43 and CP47 [6,16]. Carotenoid triplets formed by triplet transfer from chlorophylls as well as chlorophyll triplets decaying with half-lives in the ms range have been characterized by their absorbance difference spectra [6,16]. Chlorophyll triplets in CP47 and CP43 are certainly accumulated at an excitation rate above 10^4 s^{-1}. In single-molecule experiments even the decay rate of ^{3}Car at cryogenic temperatures is almost a factor of 10 lower than the excitation rate of 10^6 s^{-1} [16]. When the low energy chlorophylls in CP47 and CP43 itself are kept in the triplet state due to the high photon flux directed to the traps, the emission of these lowest lying states (e.g. F695) will be drastically reduced in the single-molecule experiment. Alternatively, it is quite possible that chlorophylls in the vicinity of the low energy states are predominantly in the triplet state. ^{3}Chl is also known to be an efficient quencher of the excitation energy [44], i.e. the emission of the low energy states might be quenched and their contribution to the fluorescence spectrum might be significantly reduced. Nevertheless, emission lines are observed in the respective spectral region; as a consequence photodamage of these chromophores can be ruled out by our single-molecule data.

As a consequence, the accumulation of triplet states in CP47 and CP43 holds the potential to change the shape of the emission spectra remarkably. In future experiments, the difference between the shape of the single-molecule average spectrum and the ensemble spectra will be used to determine the spectral characteristics of the emitters that undergo triplet formation.

The strongest reduction of the emission intensity is found for the contribution assigned to CP47 (Fig. 3). The most likely candidate for the low energy trap in CP47 is Chl29. Chl29 is located at the outside of PS II far away from the RC. At ambient conditions, the excitation transferred to Chl29 can easily be transferred back to the RC. It is interesting, why the lowest energy trap in PS II is located at the edge of PS II. One reason might be that Chl29 is a member of an additional quenching site formed by the whole photosynthetic unit including the peripheral light-harvesting complexes CP26, CP29 and LHC II. In the architecture of PS II supercomplexes of higher plants a small distance

between CP29 and CP47 was found [45]. A small distance between CP29 and CP47 could allow for efficient energy transfer between them [32].

4. Conclusion

A combination of absorption, fluorescence and low temperature single-molecule spectroscopy was used to investigate the spectral properties, heterogeneities and dynamics of the fluorescence emission of intact PS II cc from *T. elongatus*. At the ensemble level, the absorption and fluorescence spectra show a temperature dependence similar to plant PS II.

With single-molecule techniques, we are able to observe individual PS II cc. The emission spectra of these individual complexes are dominated by ZPLs showing dynamic site-energy changes. The ZPLs can be assigned to F685, F689 and F695. It is not sufficient to explain the observed spectra by assuming only one lowest trap. Single-molecule spectroscopy is especially helpful in assigning the components in the emission of PS II, because the inhomogeneous broadenings of CP43 and CP47 are responsible for the complex temperature dependence of the absorption and emission spectra of PS II. The observed spectral dynamics of ZPLs (site-energy changes) have remarkable effects on the excitation energy transfer and trapping between CP43, CP47 and the RC.

The average emission spectrum based on single PS II cc dimers shows a reduced intensity of F695 compared to reported ensemble data. The deviation can be explained by quenching of fluorescence by triplet states accumulated on Car or the red-most Chl*a* molecules like on Chl29 in CP47 induced by the excitation laser light.

Acknowledgement

This work was supported by the Heisenberg-Programm of the Deutsche Forschungsgemeinschaft DFG (BR 4102/1-1 and BR 4102/2-1) and by the DFG within the framework of the cluster of excellence on unifying Concepts in catalysis (UniCat) project B1, coordinated by the TU Berlin and Sfb 1078, project A5 (A.Z.).

References

[1] F. Rappaport, B.A. Diner, Primary photochemistry and energetics leading to the oxidation of the $(Mn)_4Ca$ cluster and to the evolution of molecular oxygen in photosystem II, Coord. Chem. Rev. 252 (3–4) (2008) 259–272.
[2] T. Renger, E. Schlodder, Optical properties, excitation energy and primary charge transfer in photosystem II: theory meets experiment, J. Photochem. Photobiol. B 104 (1–2) (2011) 126–141.
[3] Y. Umena, K. Kawakami, J.R. Shen, N. Kamiya, Crystal structure of oxygen-evolving photosystem II at a resolution of 1.9 Å, Nature 473 (7345) (2011) 55–60.
[4] A. Guskov, J. Kern, A. Gabdulkhakov, M. Broser, A. Zouni, W. Saenger, Cyanobacterial photosystem II at 2.9-angstrom resolution and the role of quinones, lipids, channels and chloride, Nat. Struct. Mol. Biol. 16 (3) (2009) 334–342.
[5] E.J.G. Peterman, H. van Amerongen, R. van Grondelle, J.P. Dekker, The nature of the excited state of the reaction center of photosystem II of green plants: A high-resolution fluorescence spectroscopy study, Proc. Natl. Acad. Sci. U.S.A. 95 (11) (1998) 6128–6133.
[6] M.L. Groot, R.N. Frese, F.L. de Weerd, K. Bromek, A. Pettersson, E.J.G. Peterman, I.H.M. van Stokkum, R. van Grondelle, J.P. Dekker, Spectroscopic properties of the CP43 core antenna protein of photosystem II, Biophys. J. 77 (6) (1999) 3328–3340.
[7] F.L. de Weerd, M.A. Palacios, E.G. Andrizhiyevskaya, J.P. Dekker, R. van Grondelle, Identifying the lowest electronic states of the chlorophylls in the CP47 core antenna protein of photosystem II, Biochemistry 41 (51) (2002) 15224–15233.
[8] J.L. Hughes, B.J. Prince, S.P. Arskold, E. Krausz, R.J. Pace, R. Picorel, M. Seibert, Photo-conversion of chlorophylls in higher-plant CP43 characterized by persistent spectral hole burning at 1.7 K, J. Lumin. 108 (1–4) (2004) 131–136.
[9] J.L. Hughes, B.J. Prince, E. Krausz, P.J. Smith, R.J. Pace, H. Riesen, Highly efficient spectral hole-burning in oxygen-evolving photosystem II preparations, J. Phys. Chem. B 108 (29) (2004) 10428–10439.
[10] E. Krausz, J.L. Hughes, P.J. Smith, R.J. Pace, S.P. Arskold, Assignment of the low-temperature fluorescence in oxygen-evolving photosystem II, Photosynth. Res. 84 (1–3) (2005) 193–199.
[11] E.G. Andrizhiyevskaya, A. Chojnicka, J.A. Bautista, B.A. Diner, R. van Grondelle, J.P. Dekker, Origin of the F685 and F695 fluorescence in photosystem II, Photosynth. Res. 84 (1–3) (2005) 173–180.
[12] M. Komura, Y. Shibata, S. Itoh, A new fluorescence band F689 in photosystem II revealed by picosecond analysis at 4–77 K: function of two terminal energy sinks F689 and F695 in PSII, Biochim. Biophys. Acta Bioenerg. 1757 (12) (2006) 1657–1668.
[13] G. Raszewski, B.A. Diner, E. Schlodder, T. Renger, Spectroscopic properties of reaction center pigments in photosystem II core complexes: revision of the multimer model, Biophys. J. 95 (1) (2008) 105–119.
[14] N.C. Dang, V. Zazubovich, M. Reppert, B. Neupane, R. Picorel, M. Seibert, R. Jankowiak, The CP43 proximal antenna complex of higher plant photosystem II revisited: modeling and hole burning study. I, J. Phys. Chem. B 112 (32) (2008) 9921–9933.
[15] B. Neupane, N.C. Dang, K. Acharya, M. Reppert, V. Zazubovich, R. Picorel, M. Seibert, R. Jankowiak, Insight into the electronic structure of the CP47 antenna protein complex of photosystem II: hole burning and fluorescence study, J. Am. Chem. Soc. 132 (12) (2010) 4214–4229.
[16] M.L. Groot, E.J.G. Peterman, I.H.M. van Stokkum, J.P. Dekker, R. van Grondelle, Triplet and fluorescing states of the CP47 antenna complex of photosystem-II studied as a function of temperature, Biophys. J. 68 (1) (1995) 281–290.
[17] P. Tamarat, A. Maali, B. Lounis, M. Orrit, Ten years of single-molecule spectroscopy, J. Phys. Chem. A 104 (1) (2000) 1–16.
[18] H.P. Lu, X.S. Xie, Single-molecule spectral fluctuations at room temperature, Nature 385 (6612) (1997) 143–146.
[19] D. Rutkauskas, V. Novoderezhkin, R.J. Cogdell, R. van Grondelle, Fluorescence spectroscopy of conformational changes of single LH2 complexes, Biophys. J. 88 (1) (2005) 422–435.
[20] F. Schleifenbaum, C. Blum, V. Subramaniam, A.J. Meixner, Single-molecule spectral dynamics at room temperature, Mol. Phys. 107 (18) (2009) 1923–1942.
[21] Y. Berlin, A. Burin, J. Friedrich, J. Köhler, Low temperature spectroscopy of proteins. part II: experiments with single protein complexes, Phys. Life Rev. 4 (1) (2007) 64–89.
[22] C. Hofmann, T.J. Aartsma, H. Michel, J. Köhler, Direct observation of tiers in the energy landscape of a chromoprotein: a single-molecule study, Proc. Natl. Acad. Sci. U.S.A. 100 (26) (2003) 15534–15538.
[23] M. Brecht, H. Studier, A.F. Elli, F. Jelezko, R. Bittl, Assignment of red antenna states in photosystem I from *Thermosynechoccocus elongatus* by single-molecule spectroscopy, Biochemistry 46 (3) (2007) 799–806.
[24] M. Brecht, H. Studier, V. Radics, J.B. Nieder, R. Bittl, Spectral diffusion induced by proton dynamics in pigment–protein complexes, J. Am. Chem. Soc. 130 (2008) 17487–17493.
[25] A.R. Faro, V. Adam, P. Carpentier, C. Darnault, D. Bourgeois, E. de Rosny, Low-temperature switching by photoinduced protonation in photochromic fluorescent proteins, Photochem. Photobiol. Sci. 9 (2) (2010) 254–262.
[26] M. Brecht, V. Radics, J.B. Nieder, R. Bittl, Protein dynamics-induced variation of excitation energy transfer pathways, Proc. Natl. Acad. Sci. U.S.A. 106 (29) (2009) 11857–11861.
[27] T.P.J. Kruger, C. Ilioaia, L. Valkunas, R. van Grondelle, Fluorescence intermittency from the main plant light-harvesting complex: sensitivity to the local environment, J. Phys. Chem. B 115 (18) (2011) 5083–5095.
[28] J. Kern, B. Loll, C. Luneberg, D. DiFiore, J. Biesiadka, K.D. Irrgang, A. Zouni, Purification, characterisation and crystallisation of photosystem II from *Thermosynechococcus elongatus* cultivated in a new type of photobioreactor, Biochim. Biophys. Acta Bioenerg. 1706 (1-2) (2005) 147–157.
[29] M. Hussels, A. Konrad, M. Brecht, Confocal sample-scanning microscope for single-molecule spectroscopy and microscopy with fast sample exchange at cryogenic temperatures, Rev. Sci. Instrum. 83 (2012) 123706.
[30] B. Loll, J. Kern, W. Saenger, A. Zouni, J. Biesiadka, Towards complete cofactor arrangement in the 3.0 Angstrom resolution structure of photosystem II, Nature 438 (7070) (2005) 1040–1044.
[31] G. Raszewski, T. Renger, Light harvesting in photosystem II core complexes is limited by the transfer to the trap: can the core complex turn into a photoprotective mode? J. Am. Chem. Soc. 130 (13) (2008) 4431–4446.
[32] Y. Shibata, S. Nishi, K. Kawakami, J.R. Shen, T. Renger, Photosystem II does not possess a simple excitation energy funnel: time-resolved fluorescence spectroscopy meets theory, J. Am. Chem. Soc. 135 (2013) 6903–6914.
[33] M. Brecht, V. Radics, J.B. Nieder, H. Studier, R. Bittl, Red antenna states of photosystem I from Synechocystis PCC 6803, Biochemistry 47 (20) (2008) 5536–5543.
[34] M. Brecht, Spectroscopic characterization of photosystem I at the single-molecule level, Mol. Phys. 107 (2009) 1955–1974.
[35] E. Krausz, J.L. Hughes, P. Smith, R. Pace, S.P. Arskold, Oxygen-evolving photosystem II core complexes: a new paradigm based on the spectral identification of the charge-separating state, the primary acceptor and assignment of low-temperature fluorescence, Photochem. Photobiol. Sci. 4 (9) (2005) 744–753.
[36] M. Hussels, M. Brecht, Effect of glycerol and PVA on the conformation of photosystem I, Biochemistry 50 (18) (2011) 3628–3637.
[37] J.P. Dekker, A. Hassoldt, A. Pettersson, H. van Roon, M.L. Groot, R. van Grondelle, On the nature of the F695 and F685 emission of photosystem II, photosynthesis: from light to biosphere, 1 (1995) 53–56.
[38] B. Hillmann, E. Schlodder, Electron-transfer reactions in photosystem-II core complexes from Synechococcus at low-temperature—difference spectrum of P680(+) Q(a)(−)/P680 Q(a) at 77 K, Biochim. Biophys. Acta Bioenerg. 1231 (1) (1995) 76–88.

[39] S. Okayama, W.L. Butler, The influence of cytochrome b 559 on the fluorescence yield of chloroplasts at low temperature, Biochim. Biophys. Acta Bioenerg. 267 (3) (1972) 523–529.
[40] F. Müh, M. Cetin, E. Schlodder, Temperature dependence of fluorescence induction in photosystem II core complexes from *Thermosynechococcus elongatus*, in: A. van der Est, D. Bruce (Eds.), Proceedings of the 13th International Congress of Photosynthesis in Montreal, Canada, International Society of Photosynthesis, 2005, pp. 309–311, (Vol.).
[41] R.H. Schweitzer, G.W. Brudvig, Fluorescence quenching by chlorophyll cations in photosystem II, Biochemistry 36 (38) (1997) 11351–11359.
[42] R. Steffen, H.J. Eckert, A.A. Kelly, P. Dormann, G. Renger, Investigations on the reaction pattern of photosystem II in leaves from *Arabidopsis thaliana* by time-resolved fluorometric analysis, Biochemistry 44 (9) (2005) 3123–3133.
[43] F. Müh, T. Renger, A. Zouni, Crystal structure of cyanobacterial photosystem II at 3.0 Å resolution: a closer look at the antenna system and the small membrane-intrinsic subunits, Plant Physiol. Biochem. 46 (3) (2008) 238–264.
[44] E. Schlodder, M. Cetin, M. Byrdin, I.V. Terekhova, N.V. Karapetyan, P700(+)- and (3) P700-induced quenching of the fluorescence at 760 nm in trimeric photosystem I complexes from the cyanobactenium *Arthrospira platensis*, Biochim. Biophys. Acta Bioenerg. 1706 (1-2) (2005) 53–67.
[45] S. Caffarri, R. Kouril, S. Kereiche, E.J. Boekema, R. Croce, Functional architecture of higher plant photosystem II supercomplexes, EMBO J. 28 (19) (2009) 3052–3063.